

On prediction of the compressive strength and failure patterns of human vertebrae using a quasi-brittle continuum damage finite element model

Zahira Nakhli, Ben Hatira, Martine Pithioux, Patrick Chabrand, Khemais Saanouni

► **To cite this version:**

Zahira Nakhli, Ben Hatira, Martine Pithioux, Patrick Chabrand, Khemais Saanouni. On prediction of the compressive strength and failure patterns of human vertebrae using a quasi-brittle continuum damage finite element model. Acta of Bioengineering and Biomechanics, Wroclaw University of Technology, 2019, 21 (2), pp.143-151. 10.5277/ABB-01265-2019-03 . hal-02291454

HAL Id: hal-02291454

<https://hal-utt.archives-ouvertes.fr/hal-02291454>

Submitted on 24 Feb 2020

HAL is a multi-disciplinary open access archive for the deposit and dissemination of scientific research documents, whether they are published or not. The documents may come from teaching and research institutions in France or abroad, or from public or private research centers.

L'archive ouverte pluridisciplinaire **HAL**, est destinée au dépôt et à la diffusion de documents scientifiques de niveau recherche, publiés ou non, émanant des établissements d'enseignement et de recherche français ou étrangers, des laboratoires publics ou privés.

On prediction of the compressive strength and failure patterns of human vertebrae using a quasi-brittle continuum damage finite element model

ZAHIRA NAKHLI^{1*}, FAFA BEN HATIRA¹, MARTINE PITHIOUX²,
PATRICK CHABRAND², KHEMAIS SAANOUNI³

¹ Laboratoire de Recherche Matériaux Mesures et Application (MMA), University of Carthage,
National Institute of Sciences and Technology (INSAT), Tunis, Tunisia.

² Aix Marseille University, (ISM) Institute of Movement Sciences, Marseille, France.

³ ICD/LASMIS, Université de Technologie de Troyes, Troyes, France.

Purpose: Damage of bone structures is mainly conditioned by bone quality related to the bone strength. The purpose of this work was to present a simple and reliable numerical treatment of a quasi-brittle damage constitutive model coupled with two different elastic modulus and to compare the numerical results with the experimental ones. *Methods:* To achieve this goal, a QCT based finite element model was developed within the framework of CDM (Continuum Damage Mechanics) and implemented in the FE code (ABAQUS). It described the propagation of brittle cracks which will help to predict the ultimate load fracture of a human vertebra by reproducing the experimental failure under quasi-static compressive loading paths of nineteen cadaveric lumbar vertebral bodies. *Results:* The numerical computations delivered by the proposed method showed a better agreement with the available experimental results when bone volume fraction related Young's modulus ($E_{(BV/TV)}$) is used instead of density related Young's modulus ($E_{(\rho)}$). Also, the study showed that the maximum relative error (%) in failure was 8.47% when $E_{(BV/TV)}$ was used, whereas the highest relative error (%) was 68.56% when $E_{(\rho)}$ was adopted. Finally, a mesh sensitivity analysis revealed that the element size has a weak incidence on the computed load magnitude. *Conclusions:* The numerical results provided by the proposed quasi-brittle damage model combined with $E_{(BV/TV)}$ are a reliable tool for the vertebrae fracture prediction.

Key words: finite element, elastic modulus, vertebrae fracture, quasi-brittle damage model, mesh sensitivity

1. Introduction

The motivation of this research was to evaluate the risk of vertebral fracture in order to provide valuable improvement for both clinicians and biomedical researchers. Accordingly, a quasi-brittle continuum damage finite element was developed and the ability of the model to predict vertebral fracture load was evaluated and compared to the experimental data.

Vertebral fractures are not only related to a fall or trauma, but are often related to the vertebrae's

microarchitectural properties such as bone density, which classify vertebrae as normal or osteoporotic. The osteoporosis that is affecting an increasing number of people (men and women) is a disease characterized by the weakness of the bones, which increases the risk of their breaking. It is an age-related disease causing progressive skeletal disorder characterized by a low bone mass, microarchitectural alterations, and an increase in bone fragility [19]. This causes pain and a significant loss of mobility for older adults. In most cases, it has been proved that osteoporotic vertebral fractures are associated with decreasing life quality [12].

* Corresponding author: Zahira Nakhli, INSAT, 676 INSAT Centre Urbain Nord BP, Cedex 1080, Tunis, Tunisia. Phone: 0021650732669, e-mail: zahira_nakhli@yahoo.fr

Clinically speaking, osteoporosis is diagnosed using dual-energy X-ray absorptiometry (DXA) [16], which measures the bone's mineral density (BMD). The fracture risk is assumed to be highly correlated with the value measured by the DXA. Osteoporosis is diagnosed if the BMD is less than 0.648 g/cm^2 (T -score less than -2.5). Osteopenia is defined for bones with a BMD between 0.833 and 0.648 g/cm^2 (equivalent to a T -score between -1.0 and -2.5). Bones are considered as normal if the BMD is above 0.833 g/cm^2 (T -score above -1.0). It is also noteworthy that DXA is subject to restrictions for the assessment of bone fragility and osteoporosis diagnosis. DXA is based on 2D and not 3D measurements and used only for porous bone information and not for compact bone. It is known that microarchitecture alteration is currently included in the definition of osteoporosis [19]. Emilie Sapin [23] recalls that BMD measurement based on this technique only accounts for 18–78% of the decrease in vertebral resistance.

Mechanical approaches based on finite element modeling have been proposed as an alternative to predict vertebral resistance. Several FE models describing damage and fractures of bone structures have been proposed in the literature [4], [15].

Quantitative computed tomography (QCT) is one of the most used techniques in these previous studies to approach the specific geometry and bone structure mechanical properties. The obtained QCT-based finite element (FE) voxel models have been presented to predict the ultimate force of human lumbar vertebrae under axial compression. The study by Chevalier et al. [4] presented a novel generation of FE models based on CT images with clinical resolution to predict the stiffness and strength of human vertebral bodies and investigate damage accumulation in a variety of loading conditions.

Mirzaei et al. [17] presented a study to predict the failure of human vertebrae based only on the strength level and failure patterns throughout the implementation of the QCT voxel-based FEM. In [6], Giambini introduced a finite element model of vertebral compression fracture analyzed with the extended finite element method. In this work, specimen-specific quantitative computed tomography QCT/X-FEM models of the lumbar vertebra (L3) were successfully created. In Schileo et al. [24], a combined experimental-numerical approach was used to build up subject-specific finite element models to accurately predict the failure patterns of bones.

In addition, over the last decades, developments in 3D have provided possibilities for measuring a variety of structural indices to characterize bone microar-

chitecture. The dependency of the microarchitecture on the bone's mechanical properties was presented by Ulrich [25]. The authors showed that the prediction of the Young's modulus is improved by supplementing BV/TV with 3D structural indices. The results presented by Morgan et al. [18] indicated that there is no universal modulus–density relationship for on-axis loading paths. The authors suggested that the site-specificity in the apparent modulus–density relationships may be attributed to the differences in architecture. For isotropic cellular materials, a basic model consists of a power relationship of the Lamé constants with respect to the bone volume fraction [7]. Additional studies found in the literature followed different approaches to estimate the Young's modulus. For example, Clouthier et al. [5] reported that the mechanical behavior of trabecular bone is mainly governed by its tissue modulus and morphology, i.e., the bone volume fraction (BV/TV), especially in the case of small strains. In the study by Kaneko et al. [11], the authors adopted elasticity-apparent density relationships to build their FE models.

Finally, dealing with the quasi-brittle damage models, one of the major works on this issue was presented by Hambli [9]. In this study, the authors presented a simple finite element (FE) analysis using a quasi-brittle damage models for the proximal femoral fracture prediction based on orthotropic assumption.

In general, most of the articles found in the literature show how important it is to provide a precise diagnosis of the fracture state (magnitude and localization), and how to establish linear or non-linear behavior, isotropic or anisotropic models to quantify the bone fracture. They also stated that the most important parameter, conditioning bone fracture in vertebral bodies, is its mechanical properties. As it is well known, the Young's modulus is a major mechanical property qualifying the strength of any elastic structure. However, they showed controversies in different conclusions on the same topic. In order to propose a new efficient numerical tool, the Continuum Damage Mechanics CDM framework was chosen to develop the isotropic quasi-brittle fracture law with two elasticity properties. The model was implemented into a user routine VUMAT in the finite element software (Abaqus). The Finite element simulations were carried out using the explicit dynamic algorithm. Numerical computations for nineteen vertebrae were compared with success to experimental fracture data.

Two Young's modulus estimations methods were presented in the next section.

2. Materials and methods

2.1. Young's modulus estimations

In the present work, two distinct investigations were used to obtain the mechanical properties (Young's modulus) of each geometrical model. The first one uses an elastic modulus proportional to the bone density ($E_{(\rho)}$) whereas the second one is based on the elastic modulus proportional to the bone volume fraction $E_{(BV/TV)}$.

- Method 1: Young's modulus estimation based on bone density

Previous studies, such as the one of Jacobs et al. [10], showed that the Young's modulus for each finite element depends on the apparent density of each bone voxel ($E = f(\rho)$), which, in turn, was calculated based on CT images. The relationship between the apparent density and CT values (HU: Hounsfield units or GV: grey values) was also calibrated. The chosen formula can be expressed as:

$$E_{(\rho)} = 3500\rho^{2.2} \quad (1)$$

This method is based on a phenomenological relationship, allowing us to assign to each element a distinct mechanical property using a direct correlation between the apparent density and Young's modulus.

- Method 2: Young's modulus estimation based on bone volume fraction

Based on the study by Benedikt et al. [1] and Morgan [18], a Young's modulus was computed for the bone structure. Indeed, as described in Eq. (2), a power law function was presented to predict the trabecular human vertebrae material properties:

$$y = ax^b, \quad (2)$$

where y is the strength or elastic modulus, x a parameter (i.e., apparent density), a and b empirical constants derived from the correlation with the experimental data. In the following relationship, the bone volume over the total volume is called (BV/TV):

$$E_{(BV/TV)} = 4730 \left(1.8 \frac{BV}{TV} \right)^{1.56} \quad (3)$$

In the following material, the experimental method and the numerical models combined with the two Young's modulus estimations are described. First, the procedure to obtain the data and geometry of the nineteen CT scanned lumbar vertebrae was introduced. As previously pointed out, the continuum damage me-

chanics (CDM) framework was chosen since it is the most appropriate constitutive framework to reproduce the bone structure failure. The boundary and load conditions used in the computation are also presented. The results of these simulations of different cases are detailed for the sake of a comparison between the theoretical and experimental results.

2.2. Sample preparation

Nineteen lumbar vertebrae (L2, L3, L4) from 7 human donors (4 females and 3 males) were CT-scanned using a GE Medical Systems scanner available in La Timone University Hospital (Marseille). DICOM images generated by the scanner were constituted by pixels with different grey intensities. The investigations were approved by the research ethics board at the University Hospital.

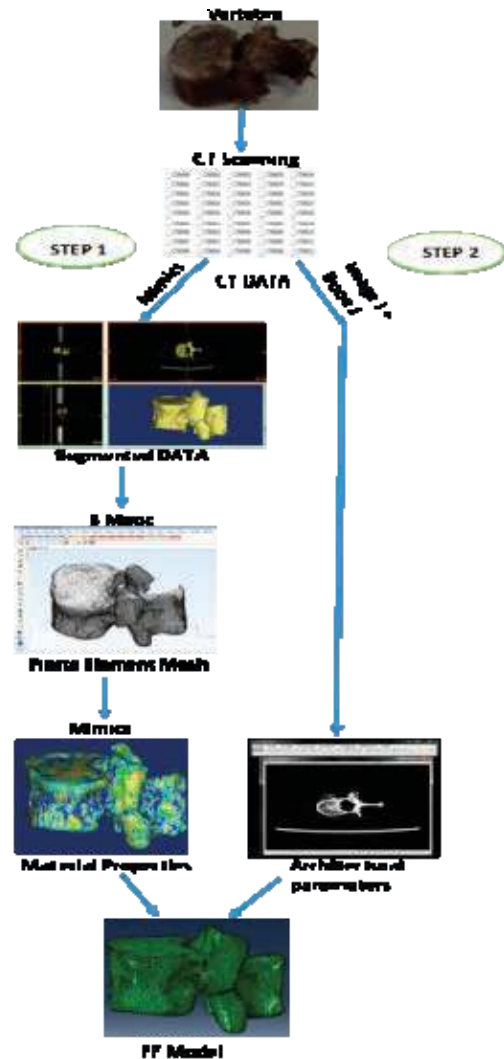


Fig. 1. Flow chart showing the protocol established to create FE models from CT data

- Step 1: 3D reconstruction was performed using the technique of density segmenting with the research software Mimics 17.0. The generation of the surface and volume meshes was done using the research software 3Matic 9.0.0.231. This was used to create a triangular mesh on the surface of the vertebra, and to generate the volume mesh with linear tetrahedral elements. The volume mesh was imported again into Mimics, in order to assign the material parameters based on the Hounsfield units (HU) or units'grey values on the scanned images; also the density ρ and the Young's modulus E were obtained at the end of this step. This elastic modulus was used in Method 1.
 - Step 2: Through the software Image J combined with the software Bone J, the architectural parameters were extracted: BV/TV (the bone volume fraction), Tb.Th (trabecular thickness), Tb.Sp (trabecular spacing) and Tb.N (trabecular number). BV/TV was used to compute the elastic modulus in Method 2.
- The flow chart summarizing the protocol established to create the FE models from CT data using material properties is presented in Fig. 1.

2.3. Experimental mechanical compression test

To reproduce the trauma due to the compression loading of nineteen cadaveric lumbar vertebrae, an INSTRON 5566 device was used. The vertebrae em-



Fig. 2. Lumbar vertebra before failure. The resin is placed at the top and the bottom of the vertebral body

bedded with common epoxy resin (average height = 6.5 mm) were placed between the jaws (Fig. 2). Epoxy resin was maintained during the entire test and enabled the vertebrae to be set in the vertical axis of the compression device. A velocity of 5.0 mm/min was imposed during the test. The load [kN] and displacement [mm] were continuously measured.

In order to reproduce the obtained experimental data, the localization of the crack, the state of damage and the ultimate load failure, a CDM model coupled with the two Young's modulus calculations was used.

2.4. Bone constitutive models

Constitutive framework:

A quasi-brittle damage model

The approach of irreversible thermodynamics with internal variables [3], [21] was chosen to present a coupled damage elastic model to describe the initiation and the accumulation of the damage in bone structure, more precisely, the vertebra.

In this work, the damage behavior model describing a quasi-brittle behavior, using an isotropic Continuum Damage Mechanics (CDM) based on Marigo [14] modeling of the damage for brittle and quasi-brittle materials, was proposed.

The new energy-based model can be described throughout state variables (external and internal). The state variables describing the constitutive equations are represented by the external or observable state variables, namely the elastic strain components ε_{ij}^e and the Cauchy stress σ_{ij} . For the sake of simplicity, damage is assumed isotropic, described by a couple of scalar internal variables (D , Y) where Y is the damage force associated to the damage variable D .

The state relationships defining the stress-strain relation of elasticity-based damage mechanics can be expressed by:

$$\sigma_{ij} = (1 - D)a_{ijkl}\varepsilon_{kl}^e, \quad (4)$$

where a_{ijkl} are the components of elasticity tensor.

$$Y = \frac{1}{2}\varepsilon_{ij}^e a_{ijkl}\varepsilon_{kl}^e. \quad (5)$$

The damage criterion (or damage yield function) can be described by the Eq. (6):

$$f(Y, D) = Y - \frac{1}{2}Y_0 - mD^s = 0, \quad (6)$$

where Y_0 , s and m are three parameters characterizing the damage evolution. Here, it was assumed that the damage yield function Eq. (6) can describe the initiation of micro-cracks starting from undamaged state ($D = 0$).

The damage evolution equation was derived to get:

$$\dot{D} = \frac{s}{m} \left(\frac{\dot{Y}}{D \left(\frac{1-s}{s} \right)} \right), \quad (7)$$

in which the time derivative of the force Y is given by:

$$\dot{Y} = \varepsilon_{ij}^e a_{ijkl} \dot{\varepsilon}_{kl}^e \quad (8)$$

According to Eq. (4), when damage increases by Eq. (7), then the stress tensor decreases due to the decrease of the Young's Modulus.

This isotropic simulation approach represents a simple numerical tool given the limited number of model parameters.

The proposed algorithm implementing the model was summarized in Fig. 3. The first step consists of the global model definition: geometry, load conditions and initial bone density distribution. The second step is concentrated on the determination of Young's modulus, Poisson's ratio and the density. These material properties are obtained by two methods as explained in previous section. The third step is related to the computation of the displacement, by solving the variational equation of the displacement field. Based on the FE method, strain, the stress and the damage are computed at each discrete location (step 4). Thereafter, an update of the stress (step 5)

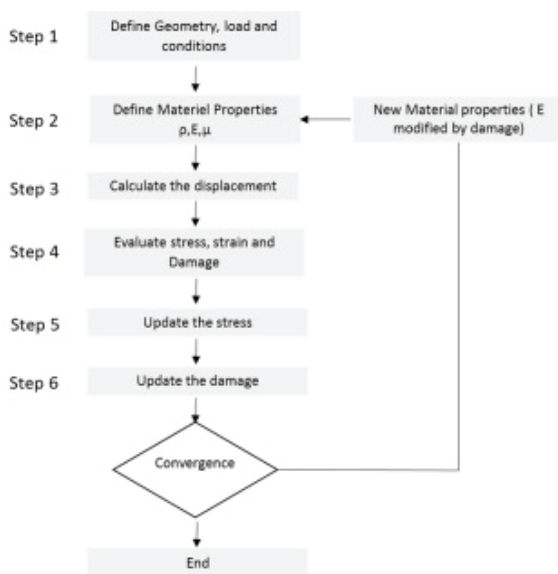


Fig. 3. Schematic representation of the Bone Damage algorithm proposed

and damage (step 6) values are applied. The model is implemented into the FE code Abaqus/Standard via the user subroutine VMAT. The final result is obtained when the convergence criterion is satisfied; otherwise, the iterative process continues from Step 2. An illustration of the algorithm used is described in Fig. 3.

2.5. Simulations

Boundary and loading conditions

In general, fracture of the vertebra occurs when the bone is subjected to a high compression load. A compressive pressure is then applied to the vertebra's upper surface embedded in resin and the lower surface is constrained in all directions (Fig. 4). The pressure value corresponds to the ratio of the failure load over the vertebra surface.

The computations were carried out using the kill element method based on the critical value of the damage variable. This method simulates the macroscopic cracks propagation direction by setting the stiffness matrix to zero when the critical damage value ($D = 0.999$) is reached inside an element of the mesh. Concerning the contact problem that may occur during these computations, Abaqus/CAE software automatically uses a general contact algorithm to avoid intersection of the damage elements. Finally, an example of the bone material properties is given in Table 1. A mean value of the BV/TV equal to 0.3, used to evaluate the $E_{(BV/TV)}$, was assigned to all the vertebrae in the computing process.

In all the studied cases, damage parameters Y_0 , m and s used in Eq. (6) have been identified in [13] based on the available experimental data and the best values of these parameters for the present material were: $Y_0 = 0.0001$, $s = 0.1$ and $m = 0.8$.

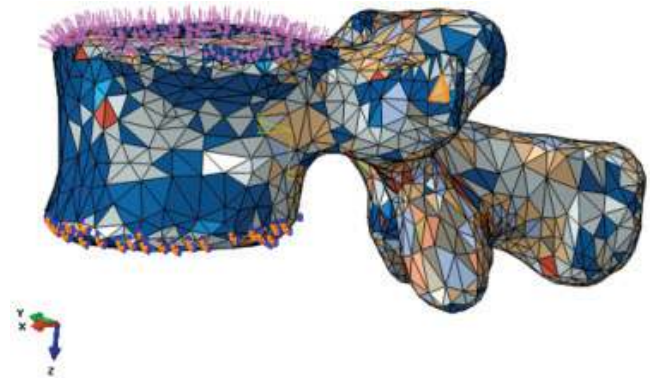


Fig. 4. Vertebra Load and boundary conditions (meshing of the specimen Sp4-L3 using 8739 linear tetrahedral elements)

Table 1

| Method 1 (for the specimen Sp4-L3) | | | | |
|------------------------------------|------------------------------|------------------------|----------------------|---------------|
| | Density (g/cm ³) | Young's Modulus (MPa) | Poisson ratio | |
| Cortical bone | 0.62-2.33 | 1215-22485 | 0.3 | |
| Cancellous bone | 0.05-0.41 | 7.36-506 | 0.3 | |
| Method 1 (for the specimen Sp6-L2) | | | | |
| | Density (g/cm ³) | Young 's Modulus (MPa) | Poisson ratio | |
| Cortical bone | 0.64-2.09 | 1330-17859 | 0.3 | |
| Cancellous bone | 0.005-0.41 | 1.03-517 | 0.3 | |
| Method 2 | | | | |
| | Density (g/cm ³) | BV/TV | Young's Modulus(MPa) | Poisson ratio |
| Vertebra | 0.05-2.33 | 0.3 | 1710 | 0.3 |

3. Results

As mentioned before, the purpose of this work was to predict effectively the damage localization as well as the ultimate fracture strength for different specimens tested experimentally and presented in the previous sections. During the conducted experiments, failure load was obtained for the nineteen vertebrae. The mean failure load was 2.744 kN. The initial crack always occurred in the middle of the vertebra. Experimental ultimate load and BMD for all vertebrae are reported in Table 2.

Table 2

| Specimen | Vertebra | BMD (g/cm ²) | Load (kN) |
|------------|-------------------|--------------------------|-----------|
| Sp1 | L2 (normal) | 1.016 | 1.615 |
| | L3 (normal) | 0.985 | 2.343 |
| | L4 (normal) | 1.015 | 2.597 |
| Sp2 | L3 (osteopenic) | 0.745 | 1.627 |
| Sp3 | L2 (normal) | 1.118 | 5.180 |
| | L3 (normal) | 1.183 | 5.266 |
| | L4 (normal) | 1.364 | 5.032 |
| Sp4 | L2 (osteopenic) | 0.749 | 1.616 |
| | L3 (normal) | 0.864 | 1.766 |
| | L4 (normal) | 0.920 | 2.806 |
| Sp5 | L2 (normal) | 0.884 | 3.501 |
| | L3 (normal) | 0.938 | 3.074 |
| | L4 (normal) | 0.881 | 2.839 |
| Sp6 | L2 (osteoporotic) | 0.616 | 1.057 |
| | L3 (osteoporotic) | 0.623 | 1.393 |
| | L4 (osteoporotic) | 0.570 | 0.878 |
| Sp7 | L2 (osteopenic) | 0.819 | 2.437 |
| | L3 (normal) | 0.969 | 3.215 |
| | L4 (normal) | 0.995 | 3.885 |
| Mean value | | 0.908 | 2.744 |

Figure 5, taken during the compression of one of the specimens, shows clearly that the failure occurs in the middle of the vertebra with a wedge fracture with a mean vertebra height reduction of 25%.



Fig. 5. Lumbar vertebra after failure. Localization of the fracture in the middle of the vertebral body

The ultimate strength load values obtained experimentally were used to compute the applied pressure for all the computing cases with the two-elastic modulus. The non-linear analysis showed that the localized damaged zones were found to be different for each method.

Predicted load-displacement curves with both methods (Method 1 and Method 2) are shown in Fig. 6a-d for two chosen specimens (Sp4-L3 (normal) and Sp6-L2 (osteoporotic)). Clearly, Method 2 gives better similarity with the experimental curves (Figs. 6b and 6d) than the Method 1, as shown in Figs. 6a and 6c.

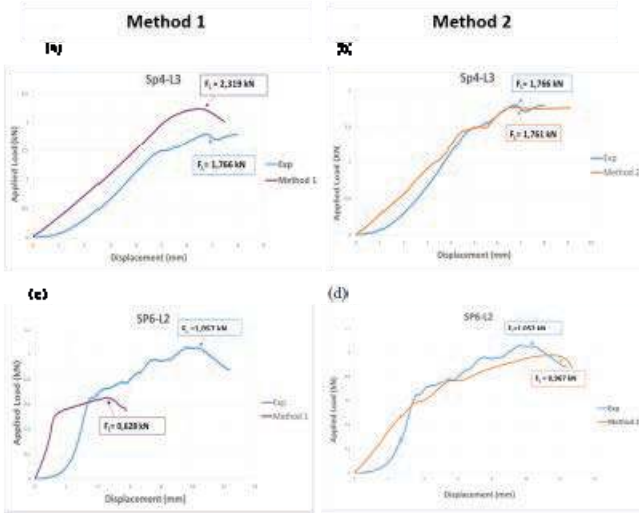


Fig. 6. Predicted and experimental force-displacement curves obtained for two vertebrae under compression

In Fig. 7a the computed ultimate loads obtained for the nineteen vertebrae based on the two methods are summarized. The relative errors δ (%) between the experimental measured and predicted compressive failure loads are indicated in Fig. 7b.

The choice of Method 2 gives good agreement with the experimental data ($0.27\% < \delta < 8.47\%$), whereas the choice of Method 1 leads to a large range of relative errors ($16.37\% < \delta < 68.56\%$) (Fig. 7b).



Fig. 7a. Experimental and computed failure loads for the nineteen vertebrae (Method 1 and Method 2)

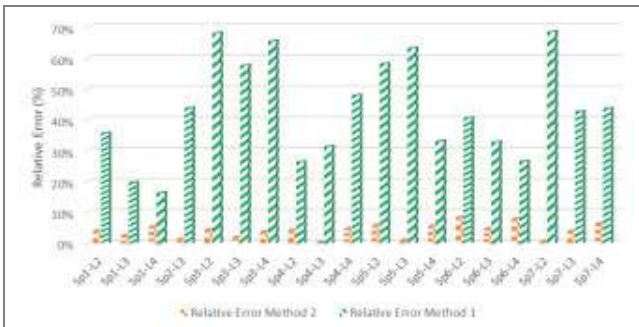


Fig. 7b. Relative Errors (%) of failure loads for the nineteen vertebrae (Method 1 and Method 2)

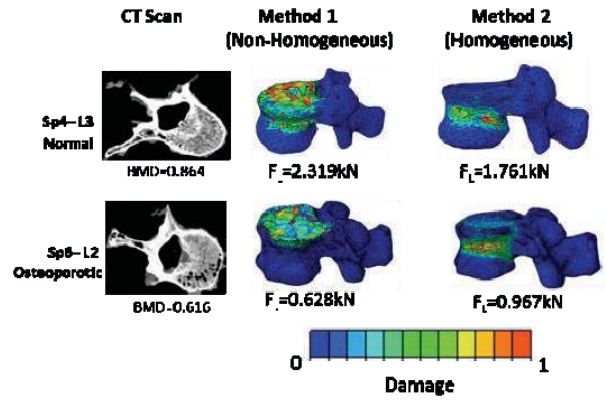


Fig. 8. CT-Scan and FE results for the two specimens: damage localization zones when the experimental failure load F_L (kN) is reached for the two methods

Concerning the predicted fracture patterns, Fig. 8 shows the state of the two chosen specimen when the ultimate experimental failure load F_L [kN] is reached for the two methods. It shows that, if we choose Method 2, the predicted fracture patterns match well with the visually observed experimental cracks for the two specimens. Indeed, in this case, the damage localization occurs in the middle of the vertebra. However, the choice of computations combined with Method 1 leads to a fracture zone located on the top of the vertebra for all computed cases which is different from the experimental results.

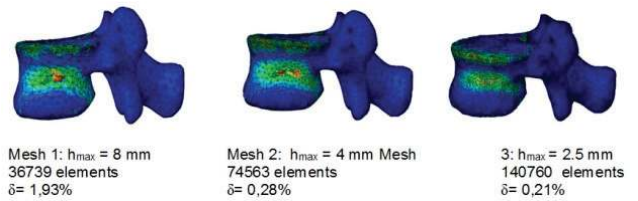


Fig. 9a. Different meshes and Distribution of the damage variable (D) for specimen Sp4-L3; h – element size

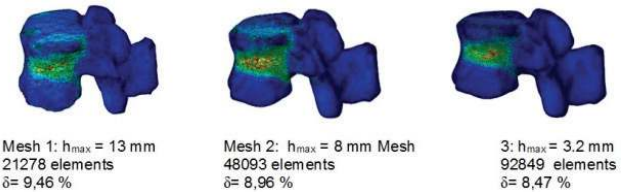


Fig. 9b. Different meshes and Distribution of the damage variable (D) for specimen Sp6-L2; h – element size

Further investigation has been performed to check the mesh dependency of the computed fracture load for the two studied specimens (Sp4-L3 and SP6-L2) with a choice of Method 2. Each vertebra was meshed with linear tetrahedral elements C3D4 using three different mesh sizes (Figs. 9a and 9b). We can see that the dis-

tribution of the damage variable D inside the two specimen is the same for the three meshes but the crack width was directly correlated to the mesh size. However, the relative error δ between the experimental and numerical failure loads were fairly acceptable for the studied cases. Indeed, the relative errors ranges were ($0.28\% < \delta < 1.93\%$) and ($8.47\% < \delta < 9.46\%$) for specimens Sp4-L3 and Sp6-L2, respectively. We can conclude as far as the magnitude failure load is concerned, the element size has a weak incidence and that our numerical model can be considered as a reliable prediction tool.

4. Discussion

The aim of this work was to develop a simple quasi-brittle method to describe the process of vertebral fracture and to compare it to the experimental ones. Constitutive equations were developed using a CDM model to be the best to fit to the experimental data.

In a study by Goulet et al. [8], the authors stated how that density measures often lead to a scalar measure inadequate for predicting the material properties. However, they proved that strong correlations are found between bone fraction (BV/TV) and elastic modulus. The results of the numerical investigation showed the capabilities of our proposed FE element modelling to describe and predict the localization of normal or osteoporotic vertebra failure based on the choice of the right elastic modulus, i.e., $E_{(BV/TV)}$.

Good quantitative and qualitative results were obtained as detailed in the preceding section. It is important to note that, in our current analysis, the assumption of a starter crack was not used, thus the origin and initiation of the crack was not forced to start at a specific region, but it rather developed naturally.

A correlation between micro and macro mechanisms is suitable to better understand the completely physical process of damage in order to enhance the damage modeling. Besides, since the continuum level is largely dependent on both size and orientation of the mesh elements, the mesh size should be accurately determined for each type of material [2]. Further studies, including a more appropriate FE meshing algorithm, are indeed necessary to treat the mesh dependency problem. In fact, numerical implementation of the quasi-brittle damage model exhibits strong spurious mesh dependency with the localization taking place over a scale defined from the discretized element size, as expected and mentioned in [20]. Mainly, in this study, the insertion of non-local variables has

proved to be an efficient way to avoid mesh sensitivity. However, this method relies on an arbitrary choice of the weighted averaging function. The use of generalized nonlocal formulations has to be applied in order to properly avoid the mesh dependency when the damage induced softening is accounted for [22].

Despite these limitations, the CDM modelling did show some real potential to correctly predict the localization of fractures as well as the failure loads for different types of vertebra (normal or osteoporotic).

5. Conclusion

The purpose of this work was to develop and validate a simple FE model based on continuum damage mechanics in order to quantify lumbar vertebra failure. This paper compared the experimental data with the numerical results using a quasi-brittle damage constitutive model coupled with two different elastic moduli. The results demonstrate that the choice of an elastic modulus related to the bone volume fraction gives the best agreement with the experimental response of vertebral bone failure under a quasi-static compression.

Nevertheless, our study has several limitations. First, the isotropic behavior law should be modified since the bone structure is known to be anisotropic. Second, the mesh dependency revealed that the damage localization crack width depends on the element size.

In general, concerning FE simulations, the combination of geometric parameters (mesh sensitivity) and material parameters (BV/TV, BMD, etc.) is the best way to obtain accurate prediction of healthy or osteoporotic bone fracture.

Acknowledgements

The project was made possible thanks to the Saint Marguerite hospital radiology team specially P. Champsaur, T. Lecorroller, and D. Guenoun for providing CT SCAN, DXA used in the current work and for procuring vertebra.

References

- [1] BENEDIKT H., EGON P., ENRICO S. et al., *Mathematical relationships between bone density and mechanical properties: A literature review 2008*, Clinical Biomechanics, 2008, 23 (2008), 135–146.
- [2] BREDBENNER T.L., NICOLETTA D.P., DAVY D.T., *Modeling damage in human vertebral trabecular bone under experimental loading*, Proceedings of the 2006 SEM Annual Conference and Exposition on Experimental and Applied Mechanics, St. Louis, Missouri, US, 2006.

- [3] CHABOCHE J.L., *Continuum Damage Mechanics: Part I and II*, J. Appl. Mech., 1988, 55, 59–79.
- [4] CHEVALIER Y., CHARLEBOIS M., PAHR D. et al., *A patient-specific finite element methodology to predict damage accumulation in vertebral bodies under axial compression, sagittal flexion and combined loads*, Computer Methods in Biomechanics and Biomedical Engineering, 2008, 477–487.
- [5] CLOUTHIER A.L., HOSSEINI H.S., MAQUER G. et al., *Finite element analysis predicts experimental failure patterns in vertebral bodies loaded via intervertebral discs up to large deformation*, Med. Eng. Phys., 2015, 37, 599–604.
- [6] GIAMBINI H., QIN X., DAESCU D.D. et al., *Specimen-Specific Vertebral Fracture Modeling: A Feasibility Study using the Extended Finite Element Method*, Med. Biol. Eng. Comput., 2016, 54 (4), 589–593.
- [7] GIBSON L.J., *The Mechanical behavior of cancellous bone*, J. Biomech., 1985, 18 (5), 317–328.
- [8] GOULET R.W., GOLDSTEIN S.A., CIARELLI M.J. et al., *The relationship between the structural and orthogonal compressive properties of trabecular bone*, J. Biomech., 1994, 27, 375–389.
- [9] HAMBLI R., BETTAMER A., ALLAOUI S., *Finite element prediction of proximal femur fracture pattern based on orthotropic behavior law coupled to quasi-brittle damage*, Medical Engineering and Physics, 2012, (34), 202–210.
- [10] JACOBS C.R., *Numerical Simulation of Bone Adaptation to Mechanical Loading*, PhD Thesis, Stanford University, Department of Mechanical Engineering, 1994.
- [11] KANEKO T.S., BELL J.S., PEJICIC M.R. et al., *Mechanical properties, density and quantitative CT scan data of trabecular bone with and without metastases*, J. Biomech., 2004, 37, 523–530.
- [12] LIPS P. VAN SCHOOR, *Quality of life in patients with osteoporosis*, Osteoporosis Int. J., 2005, 16 (5), 447–455.
- [13] MANAI M.S., *Modélisation de l'endommagement d'une structure osseuse*, PFE Instrumentation et Maintenance Industrielle, INSAT, Université de Carthage, Tunisie, 2015.
- [14] MARIGO J.J., *Formulation of a damage law for an elastic material. Comptes Rendus, Serie II – Mécanique, Physique, Chimie, Sciences de la Terre*, 1981, 1390–1312.
- [15] MARQUER H., SCHWIEDRZIK J., ZYSSET Ph.K., *Embedding of human vertebral bodies leads to higher ultimate load and altered damage localisation under axial compression*, Comput. Meth. Biomech. Biomed. Engin., 2014, 17 (12), 1311–1322.
- [16] MARSHALL D., JOHNELLO., WEDEL H., *Meta-analysis of how well measures of bone mineral density predict occurrence of osteoporotic fractures*, BMJ, 1996, 312 (7041), 1254–1259.
- [17] MIRZAEI M., ZEINALI A., RAZMJOO A. et al., *On prediction of the strength levels and failure patterns of human vertebrae using quantitative computed tomography (QCT-based finite element method)*, J. Biomech., 2009, 42, 1584–1591.
- [18] MORGAN E.F., BAYRAKTAR H.H., KEAVENY T.M., *Trabecular bone modulus–density relationships depend on anatomic site*, J. Biomech., 2003, Vol. 36, No. 78, 897–904.
- [19] PECK W.A., BURCKHARDT P., CHRISTIANSEN C., *Consensus development conference. Diagnosis, prophylaxis, and treatment of osteoporosis*, Am. J. Med., 1993, 94 (6), 646–650.
- [20] PIJAUDIER-CABOT G., BAZANT Z.P., *Nonlocal damage theory*, Journal of Engineering Mechanics, 1987, 113(10), 1512–1533, 0733–9399.
- [21] SAANOUNI K., HAMED M., *Micromorphic approach of finite gradient – elastoplasticity fully coupled with ductile damage. Formulation and computational aspects*, International Journal of Solids and Structures, 2013, 50, 2289–2309.
- [22] SAANOUNI K., FORSTER CH., BEN HATIRA F., *On the anelastic flow damage*, Int. J. Damage Mech., 1996, 140–169.
- [23] SAPIN E., *Personnalisation des propriétés mécaniques de l'os vertébral à l'aide d'imagerie à basse dose d'irradiation: prédiction du risque de fracture*, PhD Thesis, Arts et Métiers ParisTech, Paris 2008.
- [24] SCHILEOA E., TADDEIA F., CRISTOFOLINIA L. et al., *Subject-specific finite element models implementing a maximum principal strain criterion are able to estimate failure risk and fracture location on human femurs tested in vitro*, J. Biomech., 2008, 41, 356–367.
- [25] ULRICH D., VAN RIETBERGEN B., LAIB A., RUEGSEGGER P., *The ability of three-dimensional structural indices to reflect mechanical aspects of trabecular bone*, Bone, 1999, 25 (1), 55–60.